

Magnetic anisotropies in dot arrays: Shape anisotropy versus coupling

M. Grimsditch

Materials Science Division, Argonne National Laboratory, Argonne, Illinois 60439

Y. Jaccard and Ivan K. Schuller

Physics Department, University of California-San Diego, La Jolla, California 92093-0319

(Received 3 February 1998)

The magnetization and resonance frequencies of submicron Fe magnetic dot arrays are investigated using Brillouin light scattering (BLS) and magneto-optic Kerr Effect (MOKE). Large in-plane anisotropies, evident in both the BLS and MOKE results, are traced to shape anisotropies of the individual dots. The measured magnon frequencies are in good agreement with values calculated on the basis of isolated ellipsoids without interdot coupling. [S0163-1829(98)01241-7]

INTRODUCTION

It has recently become possible, using state of the art deposition and lithography techniques, to fabricate arrays of metallic "dots".¹⁻⁹ Of particular interest is the case when the dots are ferromagnetic since these systems offer the potential for technological applications. Prior to any such technological uses it is necessary to understand their fundamental properties. Special emphasis must be placed on elucidating possible coupling mechanisms between the dots which could be used to tailor the magnetic properties. Most of the investigations to date have dealt with the switching mechanism and how it is related to the domain structure within each dot.^{1-4,7,8} Although the effects of shape anisotropy in dot- and wirelike structures has received some attention,^{1,4,9} very few experiments have been successful in probing the coupling between particles or wires arranged in well-defined arrays.⁴⁻⁶ From the fourfold in-plane anisotropy, observed in the dynamic properties of a series of permalloy dots, investigated using Brillouin light scattering (BLS),^{5,6} it was concluded that a weak dipole-dipole interaction between unsaturated portions of each dot was responsible for their interaction.

We have investigated interdot coupling by studying the effect of the symmetry of the dot arrays. BLS measurements on square and hexagonal Fe arrays showed substantial two-fold anisotropies, inconsistent with these lattice symmetries. These results indicated that the dominant anisotropy in our samples is not due to interdot coupling, while SEM indicated that the noncircular nature of the dots might be its origin. By controlling the shape of the individual dots we show here that the strongest anisotropy stems from the shape anisotropy of the individual dots.

EXPERIMENTAL SETUP

The samples were prepared on Si(100) substrates using electron beam lithography and dc magnetron sputtering. The desired pattern was defined on a polymethyl-methacrylate (PMMA) resist layer and the Fe layer was sputtered on top. By a liftoff process, the PMMA is dissolved and only the Fe on the substrate remains giving the desired array of magnetic

dots. A complete description will be published elsewhere.¹⁰ All samples reported here were square lattices with a 400 nm spacing. The dots are 32 ± 2 nm thick cylinders with an elliptical base defined by a long axis a and a short axis b . The long axis a is in the range 80 to 150 nm and is rotated by an angle θ with respect to the lattice axis. The short axis b is between 60 and 120 nm resulting in different b/a aspect ratios. Figure 1 contains SEM images of two samples: one with dots close to circular (sample A) and elliptical for the second sample (sample D). Sample A has a long axis a of 90 nm with an aspect ratio b/a of 0.94 and an angle $\theta=0^\circ$, whereas sample D is characterized with $a=115$ nm, $b/a=0.78$, and $\theta=38^\circ$. In Table I we have summarized the sample sizes and shapes determined from the SEM images: typical uncertainties are 0.05 for the aspect ratios and 10° for the angle the long axis makes with the array axis.

Brillouin-scattering experiments were performed on a 3 + 2 pass tandem Fabry-Perot interferometer.¹¹ The samples were mounted with their normal along the collection axis and the incident laser beam subtended an angle of 45° to the normal; this geometry fixes the component of the magnon wave vector parallel to the surface (q) at 8.6×10^4 cm⁻¹. The magnetic field was applied in the plane of the sample and perpendicular to the wave vector of the magnon (i.e., perpendicular to the scattering plane). The samples could be rotated about the normal, thereby allowing the magnetic field to be applied along different in-plane directions. The polarization of the scattered light was analyzed at 90° to the incident polarization in order to minimize the intense signal of the unshifted laser radiation. In Fig. 2, we show a typical Brillouin spectrum from sample D in a field $H=1$ kG; the peak on the right of the spectrum is the magnon peak, the central peak is the unshifted radiation attenuated by 4×10^6 .

RESULTS AND DISCUSSION

Figure 3 shows the magnon frequency at 1 kG as a function of θ , the in-plane angle associated with a rotation about the sample normal, for four of our samples; $\theta=0^\circ$ corresponds to the two orthogonal array axes parallel to H and q , respectively. The lines in Fig. 3 are guides to the eye obtained by fitting a sine function to the data. It should be noted

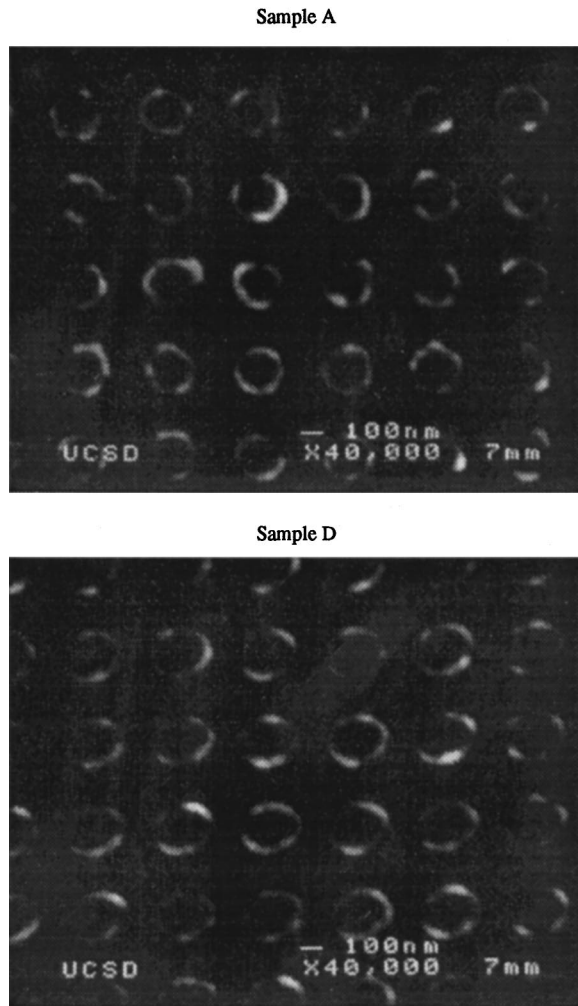


FIG. 1. SEM images of two Fe dot arrays samples A and D. Their characteristics are listed in Table I.

that a rotation about the sample normal changes both the direction of the applied field and of the wave vector relative to the dot array. It is evident from the data that some samples exhibit a substantial anisotropy. This anisotropy does not have the symmetry of the square array (90°) nor is it aligned with the array principal axes, hence it cannot be due to interdot coupling as found in Refs. 5 and 6. Its origin can be traced to the shape of the individual dots. A comparison of the sample characteristics in Table I with data in Fig. 3, shows a strong correlation between the observed anisotropies and dot aspect ratios. Furthermore, the maximum and minimum magnon frequencies occur roughly when the field is

TABLE I. Characteristics of the samples. a is the long axis, b is the short axis, c is the thickness, V is the dot volume, θ is the angle between the long axis and array axis, and d is the lattice constant of array.

	a (nm)	b (nm)	b/a	θ	c/a	V/d^3
A	90	85	0.94	0°	0.18	0.012
B	150	120	0.80	0°	0.11	0.028
C	80	60	0.75	30°	0.20	0.008
D	115	90	0.78	38°	0.14	0.016

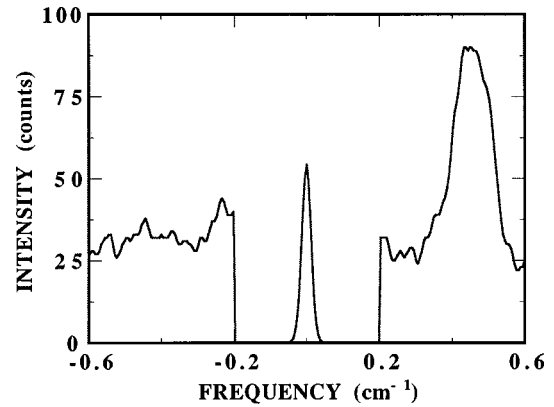


FIG. 2. Magnon spectrum obtained from sample D with an applied field of 1 kG along the easy axis. The magnon line is the peak on the right, the central peak is the unshifted radiation attenuated by 4×10^6 .

along the long and short axes of the elliptical dots, also identifying the origin of the anisotropy as due to the shape of the individual dots.

To confirm the existence of hard and easy axes, we have also measured magneto-optic Kerr loops (MOKE).¹² We remind the reader that this technique mimics magnetization loops by measuring the depolarization of a laser beam induced by changes in the magnetization direction. Loops with the field along the long and short axes of the elliptical dots of sample D are shown in Fig. 4. Because the shape favors magnetization along the long axis, the corresponding loop is typical for an easy axis; the observed hysteresis may be a reflection of the domain structure during switching at low fields. When H is applied along the short axis the magnetization rotates continuously until it is aligned along the short axis and shows no clear hysteresis. From this loop one can estimate the anisotropy to be around 1 kG. These MOKE loops therefore confirm the existence of hard and easy axes along two orthogonal directions which do not coincide with the array axes, but with the principal axes of the individual dots.

For a quantitative analysis of magnon frequencies we describe the magnons as due to the resonances of individual

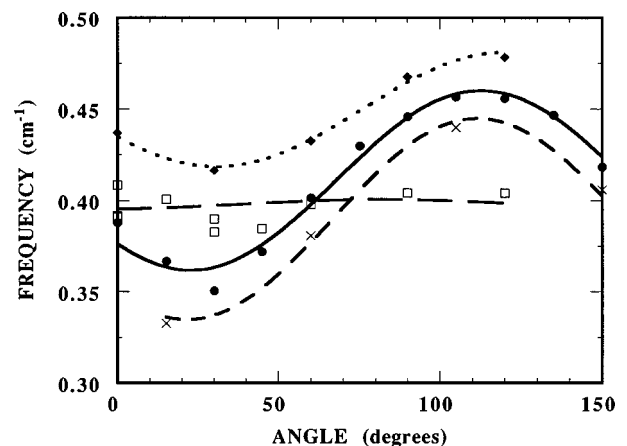


FIG. 3. Angular dependence of the magnon frequencies in a field of 1 kG. Samples A–D are indicated by open squares, rhombs, crosses, and circles respectively.

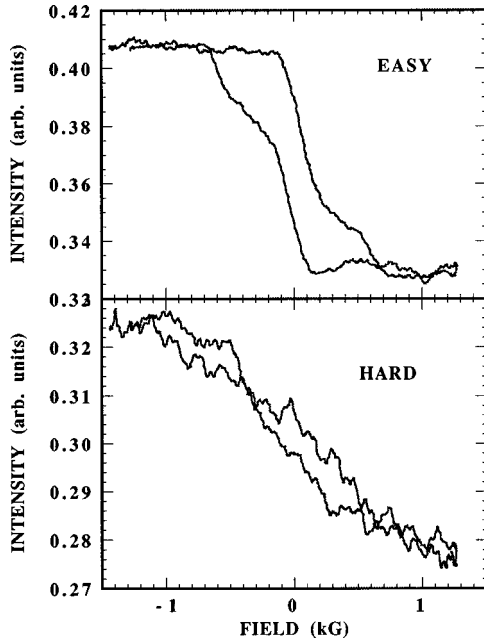


FIG. 4. Kerr loops for sample D with the field along the easy and hard axes.

ellipses.¹³ References 5 and 6, on the other hand, fitted the magnon frequencies to expressions for “surfacelike” magnons in thin magnetic films. It should be noted that both descriptions are approximations and, at this stage, until a full theoretical treatment of the dot array becomes available, it remains a matter of choice. Moreover, in the limit of thin dots with diameters large compared to the magnon wavelengths, both approaches are identical and hence the choice of formalism is probably not critical. For a field along the z direction coinciding with one of the principal axes of an ellipsoid, the fundamental resonance frequency (ω) is given¹³ by

$$\omega^2 = \gamma^2 \{ [H + 4\pi(N_y - N_z)M][H + 4\pi(N_x - N_z)M] \}, \quad (1)$$

where M is the magnetization, H is the applied field, γ is the gyromagnetic ratio (2.93 GHz/kG), and N_i ($i = x, y, z$) are the appropriate demagnetizing factors. This equation ignores interaction between dots, and assumes no *intrinsic* anisotropy within each dot. The interaction between dots, discussed quantitatively below, implies that its effect is smaller than the shape anisotropy. Intrinsic crystalline anisotropy is also likely to be small because each dot is polycrystalline and hence has no preferential axis. The remaining assumption is that we indeed observe the fundamental resonance and not one of the higher “spin-wave”-like modes. Because the wave vector probed in our experiments corresponds to a wavelength 728 nm, which is larger than the dot diameter (<200 nm), this assumption also appears to be reasonable.

In Fig. 5 we have plotted the field dependence of the magnon modes in the samples with: (a) almost circular (sample A) and (b) elliptical dots with aspect ratio 0.78 (sample D). For circular dots and defining the x axis along the surface normal, $N_y - N_z$ is zero leaving only one fitting parameter. The full line in Fig. 5(a) is the best fit yielding $4\pi(N_x - N_z)M = 16$ kG. For the sample with elliptical dots

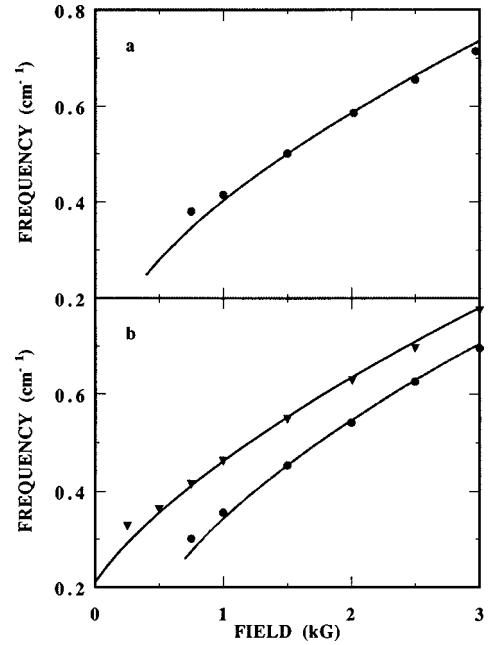


FIG. 5. Field dependence of magnons in (a) sample A, and (b) Sample D with the field along the easy and hard axes. Symbols are experimental data, lines are fits using Eq. (1).

data with the field along the hard axis (\bullet), or along the easy axis (\blacktriangle) were recorded. In this case Eq. (1) contains two fitting parameters (recall that $N_x + N_y + N_z = 1$) which must account for the magnon frequencies along the hard and easy axes. The full lines in Fig. 5 are the fit according to Eq. (1), the resulting fit parameters are: $4\pi(3N_x/2 - 0.5)M = 16.3$ kG and $4\pi(N_y - N_z)M = 0.28$ kG.

The parameters obtained from the fits in Fig. 5 can be used to extract and compare to known demagnetizing factors for ellipsoids.¹⁴ Assuming $4\pi M \approx 20$ kG (slightly lower than bulk Fe but typical for thin Fe films) leads to $N_x - N_z = 0.8$ for the circular dots, and $N_x = 0.88$ and $N_y - N_z = 0.014$ for the elliptical dots. Since the demagnetizing factors must satisfy $N_x + N_y + N_z = 1$ and $N_y = N_z$ for circular dots, this leads to the experimental values summarized in Table II. On the other hand using the dots thickness $t = c$ as the third axis of an ellipsoid with axes a, b, c we obtain¹⁴ the calculated N_i values given in Table II. Although there is qualitative agreement between calculated values and those extracted from the Brillouin results, the differences between them are larger than rough error estimates would indicate.

The discrepancies in Table II cannot be attributed to the chosen value of $4\pi M$ since to improve agreement a value larger than that of bulk Fe would be required. They may in

TABLE II. Demagnetizing factors of Fe dots estimated from Brillouin measurements and calculated from the geometry of the dots (Ref. 14).

		N_x	N_y	N_z
Experimental	Sample A	0.86	0.07	0.07
	Sample D	0.88	0.07	0.05
Calculated	Sample A	0.78	0.11	0.11
	Sample D	0.81	0.11	0.08

part be due to the approximations made in treating the dots as ellipsoids or to partial oxidation of the Fe which changes the effective aspect ratio. More interestingly they could also be an indication of interdot coupling. Great care must be taken dealing with this issue: the dipole interaction leads to an antiferromagnetic (AF) ground state¹⁵ when the dipoles are aligned out of plane while it is ferromagnetic for a square or hexagonal lattice when the dipoles lie in plane. In this latter case, however, the coupling is isotropic in-plane and hence has no effect on the magnetization.^{5,6} It is not surprising therefore that Ref. 4 did not observe the AF transition for in-plane dipoles.

To discuss the effect of dipolar coupling on the static magnetization, each dot can be viewed as a dipole of moment $p = MV$ where V is the volume of a dot. The position of each dot can be defined as $(j\mathbf{y} + k\mathbf{z})d$ where j and k are integers, \mathbf{y} and \mathbf{z} are unit vectors along y and z , and d is the lattice spacing. The field at a dot located at the origin, generated by all other dots, is given by¹⁶

$$B_y = \sum [3(j^2 p_y + jk p_z) - (j^2 + k^2) p_y] / [d^3 (j^2 + k^2)^{5/2}]. \quad (2)$$

An equivalent expression is valid for B_z , and a slightly modified equation can also be written for B_x perpendicular to the surface and the inclusion of p_x (this last expression leads to the AF ground state discussed in Ref. 15). Contrary to the case of a three-dimensional lattice, the above sums do not vanish for a two-dimensional array of dots. If all dipoles are aligned along z , far from edges of the array, Eq. (2) yields $B_y = 0$ and $B_z = 4.2 \text{ MV}/d^3$. For the samples studied here this implies $0.05 < B_z < 0.19 \text{ kG}$. Although this is a substantial field, it is isotropic in plane and hence has no effect on the in-plane magnetization. Therefore it is not possible to extract dipolar interdot coupling from magnetization loops of in-plane magnetized dots. If anisotropic effects are observed they are due to higher-order coupling or possibly array-shape anisotropy as discussed below.

The isotropy of the in-plane dipolar coupling is broken near the edges of a finite array. For example, in a 6×6 array we calculated the dipolar field at a corner by summing j, k from 0 to 5, at the center dots by summing from -2 to $+3$, etc. Figure 6 shows the dipolar field at each lattice site of a 6×6 array when the dipoles are aligned along an edge or a diagonal. When aligned parallel to an edge there is almost no tendency for the dots to misalign from the initial direction while when the field is along the diagonal, the edge dots have an effective $\approx 0.05 \text{ kG}$ field tending to misalign them. For a finite array this edge effect may lead to an apparent fourfold anisotropy. Accounting for the fraction of edge dots we expect its average value to scale as $\approx 4/n$ for an $n \times n$ array. In our samples with $n = 120$ the resulting magnitude of this ‘‘array-shape’’ coupling is 0.002 kG , considerably smaller than the $\approx 0.5 \text{ kG}$ dot-shape anisotropies discussed above. We note that this finite array anisotropy does not appear to be large enough to explain the observed fourfold anisotropy reported in Refs. 5 and 6.

Another noteworthy feature of dipole coupling is the effect of lattice symmetry. A simple generalization of Eq. (2) shows that for a rectangular lattice with $a > 2b$ the in-plane

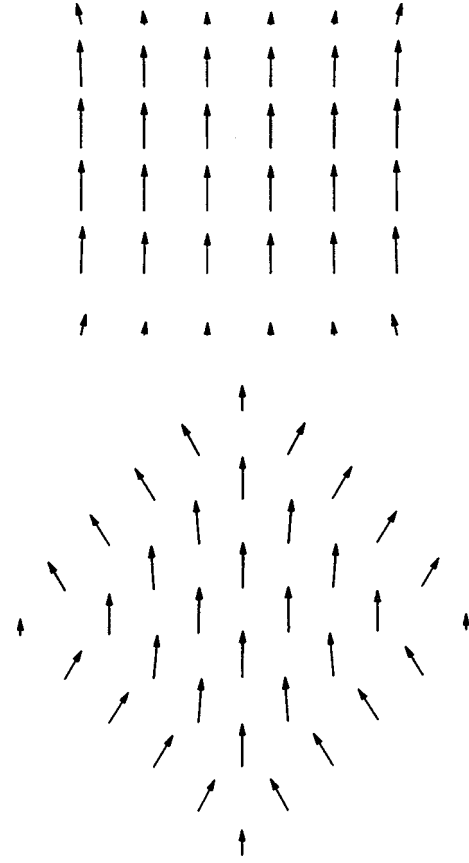


FIG. 6. Dipolar field (induced by all other dipoles in the array) at each lattice site. In (a) all dipoles are aligned parallel to an edge, in (b) along the diagonal.

dipolar field changes sign along a and b axes: i.e., it is negative when the dipoles are aligned along the long axis. This indicates that such an arrangement is unstable. If a 90° reorientation is inhibited by a shape anisotropy, such a system will have an antiferromagnetic ground state and may possess some properties such as the surface spin flop recently found in ‘‘one-dimensional’’ AF superlattices.¹⁷

The final issue which remains to be discussed is the effect of dipolar coupling on the magnon frequencies. If each dot is assumed to precess independently from all others, the field seen by each dot is an additional mean (parallel to the applied field) of $\approx 4.2 \text{ MV}/d^3$. In the other limit, when all dots precess in phase, there is no in-plane coupling but there may be a contribution perpendicular to the plane. A full solution of this problem, including the relative precession-phase in each dot, most likely results in a band of frequencies. Wave-vector conservation determines which modes within this band couple in a Brillouin experiment. It is clear that in either limit, in- or out-of phase dot precession, the magnon frequencies are independent of in-plane angle.

The different conclusion reached this work (i.e., that dot shape is the leading source of in-plane anisotropy) and that presented in Refs. 5 and 6 (i.e., that interdot coupling is responsible for the observed anisotropy) call for some speculation as to how the results of the two investigations can be reconciled. Neither the dot shape nor the array size, as discussed above, are capable of explaining the fourfold anisotropy reported in Refs. 5 and 6. As such our results cannot be interpreted as an alternative explanation of their results. Fur-

ther work on dot arrays with different symmetries, dot sizes including arrays where the dots “touch each other” along the array axes, and different substrate symmetries are still needed to fully understand the magnetic behavior of dot arrays.

CONCLUSIONS

We have shown using Brillouin scattering that the shape anisotropy of individual dots in Fe dot arrays is the dominant source of anisotropy for both the static magnetization and the resonance modes. Treating the system as isolated ellipsoids leads to good agreement with the experimental results, al-

though it is clear that details of dipolar coupling require a more complete formulation. Semiquantitative arguments indicate that, by controlling the shape of the dots and varying the lattice symmetry, it should be possible to tailor the magnetic ground state of arrays of magnetic dots.

ACKNOWLEDGMENTS

Work at ANL supported by the U.S. Department of Energy, Basic Energy Sciences, under Contract No. W-31-109-ENG-38, and at UCSD by the U.S. Department of Energy. Y.J. thanks the Swiss National Science Foundation for support. We thank J. I. Martin for useful discussions.

-
- ¹J. F. Smyth, S. Schultz, D. R. Fredkin, D. P. Kern, S. A. Rishton, H. Schmid, M. Cali, and T. R. Koehler, *J. Appl. Phys.* **69**, 5262 (1991).
- ²S. Y. Chou, P. R. Krauss, and L. Kong, *J. Appl. Phys.* **79**, 6101 (1996);
- ³M. Hehn, K. Ounadjela, J.-P. Bucher, F. Rousseaux, D. Decanini, B. Bartenlian, and C. Chappert, *Science* **272**, 1782 (1996).
- ⁴C. Miramond, C. Fermon, F. Rousseaux, D. Decanini, and F. Carcenac, *J. Magn. Magn. Mater.* **165**, 500 (1997).
- ⁵C. Mathieu, C. Hartmann, M. Bauer, O. Büttner, S. Riedling, B. Roos, S. Demokritov, B. Hillebrands, B. Bartenlian, C. Chappert, A. Müller, B. Hoffmann, and U. Hartmann, *J. Appl. Phys.* **81**, 4993 (1997).
- ⁶C. Mathieu, C. Hartmann, M. Bauer, O. Büttner, S. Riedling, B. Roos, S. Demokritov, B. Hillebrands, B. Bartenlian, C. Chappert, D. Decanini, F. Rousseaux, E. Cambriil, A. Müller, B. Hoffmann, and U. Hartmann, *Appl. Phys. Lett.* **70**, 2912 (1997).
- ⁷H. Takeshita, Y. Suzuki, H. Akinaga, W. Mizutani, K. Tanaka, T. Katayama, and A. Itoh, *Appl. Phys. Lett.* **68**, 3040 (1996).
- ⁸M. Löhndorf, A. Wadas, G. Lütjering, D. Weiss, and R. Wiesendanger, *Z. Phys. B* **101**, 1 (1996).
- ⁹S. M. Cherif and J.-F. Hennequin, *J. Magn. Magn. Mater.* **165**, 504 (1997).
- ¹⁰J. I. Martin, Y. Jaccard, A. Hoffmann, J. Nogues, J. M. George, J. L. Vicent, and Ivan K. Schuller, *J. Appl. Phys.* **84**, 411 (1998).
- ¹¹J. Sandercock, in *Light Scattering in Solids III; Topics in Applied Physics*, edited by M. Cardona and G. Güntherodt (Springer, Berlin, 1982), Vol. 51.
- ¹²S. D. Bader, *J. Magn. Magn. Mater.* **100**, 440 (1991).
- ¹³C. Kittel, *Introduction to Solid State Physics* (Wiley, New York, 1971).
- ¹⁴J. A. Osborn, *Phys. Rev.* **67**, 351 (1945).
- ¹⁵M. Goldman, *Phys. Rep., Phys. Lett.* **32C**, 1 (1977).
- ¹⁶J. Jackson, *Classical Electrodynamics* (Wiley, New York, 1962).
- ¹⁷R. W. Wang, D. L. Mills, E. E. Fullerton, J. E. Mattson, and S. D. Bader, *Phys. Rev. Lett.* **72**, 920 (1994).